Numerical Experiments of Meiyu(Baiu) Rainfall by Quasi-Lagrangian Limited Area Model with Terrain①

Zhao Li (赵 力) and *Zhao Sixiong* (赵思雄)
Institute of Atmospheric Physics, Chinese Academy of Sciences, Beijing 100080
Received July 6, 1994; revised July 25, 1994

ABSTRACT

In this paper, a 10-level Quasi-Lagrangian Limited Area Model is used to simulate the process of Meiyu(Baiu) front of 1979. Some physical processes, such as large-scale condensation and cumulus convection, are included in the model. The simulation results are encouraging. 24-h numerical simulation shows that the invading of cold air from North China and rapidly northward moving of warm air from South China can be successfully reproduced. The terrain with a maximum of 4175 m is incorporated in the model. Three different kinds of terrain schemes are tested and the dynamic effect of the Plateau on the process of heavy rainfall is found to be very important.

Key words: Meiyu, Rainband, Quasi-lagrangian, Model

I. INTRODUCTION

Some researchers have developed limited area models, e. g., Anthes and Warner(1978), Perkey(1976), Zhou et al. (1982) and so on. It should be pointed out that there has been great progress in the field of the limited area numerical prediction since 1970s. All above-mentioned models employ Eulerian prediction schemes. It has been shown that in Eulerian schemes the finite difference technique may lead to nonlinear instability when applied to the advective terms of the prediction equations. For this reason, spatial smoothing or special filters are used to control the erroneous amplification of very short waves. Sometimes, Arakawa's scheme is adopted to prevent nonlinear instability. However another way, taken by Mathur (1983), Ritchie (1985), Robert et al. (1985), Staniforth et al. (1986) and so on, of preventing the spurious growth of the meteorological variables is to use a Lagrangian scheme.

A number of analyses have been carried out to understand Meiyu front and Meiyu rainband. It has been recognized that Meiyu rainfall is produced by occurring and developing of convective clusters in the warm and cold air confluent zone under the favourable circulation condition in East Asia an the summer. However, the relation between Meiyu system and the Tibetan Plateau is not well understood so far.

Numerous GCM integrations have been carried out to investigate the orographic effects on the large-scale features. Kasahara and Washington (1971) found that the dynamic effect of mountains appeared to be less important than their thermodynamic effect and that the inclusion of mountains did not significantly alter the distribution of precipitation. However, Manabe and Terpstra (1974) concluded that the probaility of cyclogenesis increases

①This research work is financially supported by the Eighth National Five- Year Scientific Project (85-906-04-02) and National Natural Science Foundation of China(49275240).

significantly on the lee side of the mountains and that the mountains greatly affect the global distribution of precipitation. Wang and Orlanski (1987) studied a heavy rain vortex that formed over the eastern flank of the Tibetan Plateau and manifested the dynamic and thermal influences of the Tibetan Plateau.

The major purpose of the present numerical study is to simulate a Meiyu process with a Lagrangian scheme and to study terrain effects on Meiyu process. Furthermore, we try to clarify the physical processes responsible for Meiyu rainfall.

II. BRIEF DESCRIPTION OF THE MODEL

The numerical model employed in the present study is a 10–level Quasi–Lagrangian Limited Area Model(QLLAM). The main characteristics have been described at length by Muther(1983). The main characteristics of the model are reserved, and the present model has been amended neccesarily. The Tibetan Plateau terrain with the maximum of 4175 m is incorporated in the model. For the consistency between surface pressure and terrain, a second–order polynomial fitting is utilized.

The main purpose of this scheme is to avoid nonlinear instability out of differencing advective term.A special feature of this scheme is that it accounts for changes in accelerations of dependent variables and advecting velocity over the trajectory traced by the parcel in time step Δt. The inclusion of this formulation of the advective process should give the accurate prediction of the phase and amplitude of rapidly developing disturbances.

The equations of horizontal motion are

$$\frac{Du}{Dt} = A = \left[f + V\frac{\partial m}{\partial x} - u\frac{\partial m}{\partial y}\right]v - \dot{\sigma}\frac{\partial u}{\partial \sigma} - m\frac{\partial \varphi}{\partial x} - mC_p\theta\frac{\partial \pi}{\partial x} + F_{u\sigma} \tag{1}$$

and

$$\frac{Dv}{Dt} = B = -\left[f + V\frac{\partial m}{\partial x} - u\frac{\partial m}{\partial y}\right]u - \dot{\sigma}\frac{\partial v}{\partial \sigma} - m\frac{\partial \varphi}{\partial y} - mC_p\theta\frac{\partial \pi}{\partial y} + F_{v\sigma} \ . \tag{2}$$

The thermodynamic equation is

$$\frac{D\theta}{Dt} = C = -\dot{\sigma}\frac{\partial \theta}{\partial \sigma} + \frac{\theta}{C_p T} + F_{\theta\sigma} \ . \tag{3}$$

The water vapor mixing ratio is

$$\frac{Dq}{Dt} = D = -\dot{\sigma}\frac{\partial q}{\partial \sigma} + M + F_{q\sigma} \ . \tag{4}$$

The equation of continuity is

$$\frac{D\ln P_s}{Dt} = E = -\nabla_\sigma \cdot \vec{V} - \frac{\partial \dot{\sigma}}{\partial \sigma} \ . \tag{5}$$

The hydrostatic relation is

$$\frac{\partial \varphi}{\partial \sigma} = -\frac{RT}{\sigma} = -C_p\theta\frac{\partial \pi}{\partial \sigma} \ . \tag{6}$$

The poisson's equation is

$$\frac{T}{\theta} = \left(\frac{P}{P_0}\right)^{\frac{R}{C_p}} = \pi \ . \tag{7}$$

The vertical coordinate is

$$\sigma = \frac{P - P_{top}}{P_s - P_{top}}, \tag{8}$$

where P_{top} is pressure at the top of the model atmosphere. In addition, u and v are components of wind in x and y directions,respectively. θ is potential temperature, φ, geopotential height, T temperature; H is diabatic rate of heating and D/Dt is horizontal total derivative; M is rate of accession of moisture.

Simpler physical processes are included in the model, for example, nonconvective and convective release of latent heat (Kuo, 1965). The second order finite difference formula is used to evaluate all horizontal difference terms in the right hand side of Eqs.(1) to (5). The vertical advective terms are evaluated in their equivalent flux forms. After A, B, C, D and E in these equations are evaluated, the model is integrated using a one–step Quasi–Lagrangian second–order scheme. The prediction with the Quasi–Lagrangian scheme is easier to interpret physically and the advective and forcing processes are evaluated with a higher order accuracy than in the Eulerian scheme. The essence of this method is to determine at time t the position of the air partical which will arrive at a particular gridpoint at the future time $t + \Delta t$. The predicted value of a conservative meteorological variable at that gridpoint at $t + \Delta t$ is then simply taken to be the value at the previous position of the particle,as obtained by interpolation. Then, 9–point Lagrangian interpolation formula is adopted.

III. TREATMENT OF TERRAIN

Steep orography usually gives rise to errors in the coordinate evaluation of the horizontal pressure force. Therefore, the treatment of the terrain is a very important problem. For the consistency between various meteorological parameters, especially, surface pressure and temperature fields, the following second–order polynomial form is utilized:

$$\varphi(Z) = \varphi(\overline{Z}) + A(Z - \overline{Z}) + \frac{B}{2}(Z - \overline{Z})^2, \quad Z_a < Z < Z_b$$

$$A = \frac{\varphi(Z_b) - \varphi(Z_a)}{Z_b - Z_a},$$

$$B = -R\frac{T(Z_b) - T(Z_a)}{Z_b - Z_a},$$

$$\overline{Z} = \frac{1}{2}(Z_a + Z_b),$$

and $\varphi(\overline{Z})$ is geopotential height at surface. When $\overline{Z} = \ln P_s$, P_s can be computed easily.

Then, modified P_s and Z are consistent to each other.

Because of the complexity of terrain in East Asia, the C_d varying with topograph is used as follows:

$$C_d = \begin{cases} 1.3 \times 10^{-3}, & \text{ocean} \\ \left(\dfrac{6.7 \times \overline{Z}}{4175} + 1.3\right) \times 10^{-3}, & \text{land} \end{cases}$$

IV. SIMULATION WITH FGGE DATASET

The computational domain is bounded by latitudes of 10°N and 60°N and longitudes

55°E and 150°E. The horizontal array contains 79 points in zonal direction and 67 points in meridional direction with a grid size of 90km. The integration time step is 4 minutes. Ten levels are used in a σ–coordinate. These layers are selected at $\sigma=0.979$, 0.926, 0, 852, 0.704, 0.502, 0.370, 0.310, 0.250, 0.190 and 0.081.

Table 1. Numerical Simulation Schemes

EXP.1	control run
EXP.2	same as EXP.1 except for the absence of the topographical effects
EXP.3	same as EXP.1 except for using the one–third of terrain
EXP.4	same as EXP.1 except for the absence of large scale condensation
EXP.5	same as EXP.1 except for the absence of convective release of latent heat
EXP.6	same as EXP.1 except for the absence of vertical turbulent exchanges in the lower troposphere and boundary layer

To simulate the process of Meiyu front on July 8–9, 1979, NMC terrain is used. The FGGE data with an interval of 1.875° are interpolated from p–layers to σ–layers. The six experiments are conducted as in Table 1. The first experiment is control run. In the control simulation, the topographical effects, and the physical processes including large–scale condensation, convective release of latent heat, vertical turbulent exchanges in the lower troposphere and boundary layer, are incorparated. FGGE dataset is used to initialize the model at 0000 GMT 8 July 1979 and to provide a 24–h prediction. In order to study factors and physical processes related to the prediction, the results of the six experiments are given in the next section.

V. SIMULATION RESULTS

1. *Control Run*

In control run, the main features of geopotential height field have been reproduced successfully. Shown in Fig. 1a is the observed 400 hPa geopotential height. First, it is noted that the Plateau is controlled by a continental subtropical high. A westerly short wave trough is located between the Bohai Sea and the Great Bend of the Yellow River. Western Pacific subtropical high (WPSH) presides over the East China Sea and its coast, with an intensity of 7550 m. In lower latitudes, a low persists over the South China Sea, and its central value drops to 7470 m. Besides, the Indian subcontinent and the Bay of Bengal are dominated by a low pressure system with a minimum of 7460 m.

Fig. 1b illustrates the corresponding prediction field.As shown in Fig. 1b is a general agreement between the predicted and the observed fields. Main part of westerly trough arrives at the eastern coast. WPSH persists over the East China Sea with a maximum of 7550 m. The South China Sea low's intensity changes slightly at about 7480 m. The Indian low has an intensity of 7460 m. It is noted that the subtropical high over the Plateau seems to be in disagreement. There is a low value area over the central Plateau, which may be caused by strong convergence over the Plateau.

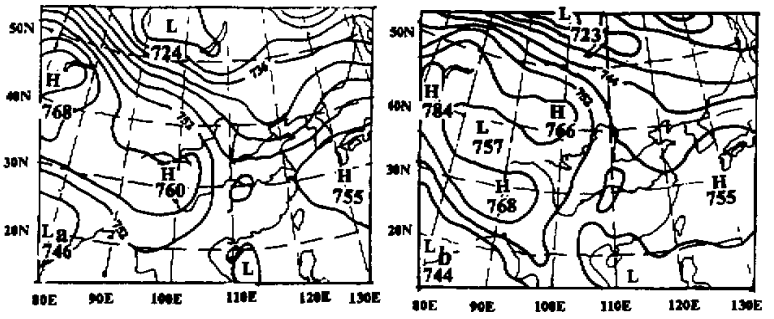

Fig. 1. 400 hPa 24h temperature field: (a) observed, and (b) predicted from the model with terrain.

2. *Comparative Experiment for the Terrain Effect*

Another experiment has been designed by removing the Plateau terrain from the model. Because of remarkable dynamic and thermal effects of the Plateau on atmospheric circulation, removing the Plateau terrain does not mean removing all these effects out of initial data. In this experiment, we use FGGE data on isobaric levels as the initial data and get 24h predictions. Fig. 2 shows the geopotential height simulated from Exp.2. It is noted that westerly short wave trough positions are located between west Japan and north China. The South China Sea low and Indian low are also reproduced successfully. However a high pressure ridge controls the Great Bend of the Yellow River and middle and lower valley of the Yangtze River and a closed center of 7540 m extends to the upper reaches of the Yellow River. This feature is not favourable for Meiyu occurrence. On the other hand, the Plateau area is covered by an intense trough. We may conclude that if there were not Tibetan Plateau, summer rainfall in China would not be concentrated in the Yangtze River valley. This means Meiyu rainband would not show up and even in the Plateau area there would be much precipitation.

3. *Experiment for the One–third of the Terrain (Exp.3)*

In Exp.2, the total terrain is removed. Obviously this may be unreasonable. Therefore, Exp.3 is designed to test the effect of the lower terrain and the one–third of terrain is incorporated in the model. The experimental results are shown in Fig.3 and the positions of the

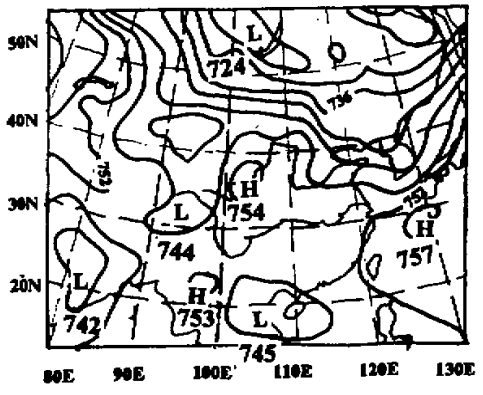

Fig. 2. 400 hPa temperature field predicted from the model without terrain.

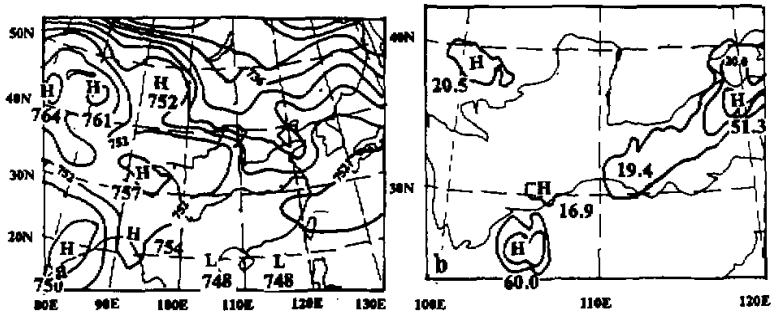

Fig. 3. 24h test field from the model with 1 / 3 terrain at 700 hPa (a) height and (b) rainfall.

troughs and ridges in East Asia are closer to the observations than those without terrain. However, the rainfall area is not so good as those with total terrain. It indicates again that the effects of the terrain are important and the authentic terrain scheme seems to be very necessary for the numerical simulation and prediction of the heavy rainfall.

4. *Experiment for the Meiyu Rainband*

Fig. 4a depicts the observed 24h accumulated precipitation(mm). A remarkable characteristic is a rainband extending SW–NEward with a maximum of 146 mm. Another precipitation area is presented to southeast of the Plateau and its maximum is 40 mm. The third precipitation area is also found in the upper reaches of the Yellow River.

Shown in Fig. 4b is the predicted precipitation whose areas agree with the observed. The rainband can be found clearly in the Yangtze River but slightly southwest diverged. On the

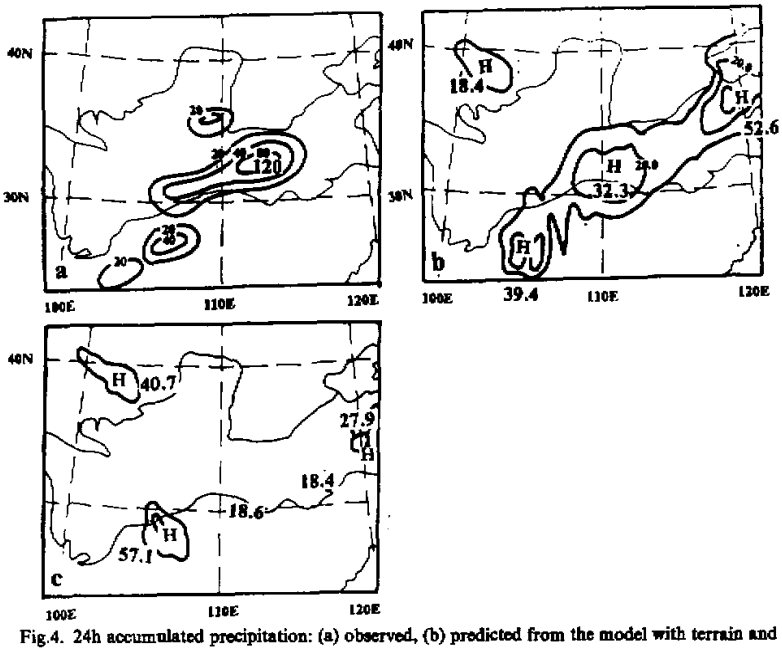

Fig.4. 24h accumulated precipitation: (a) observed, (b) predicted from the model with terrain and (c) predicted from the model without terrain.

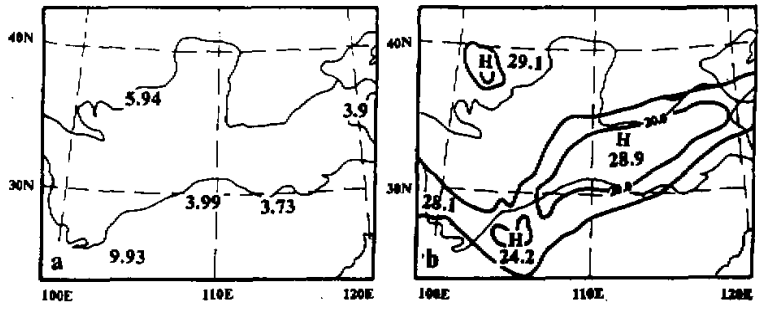

Fig. 5. Predicted 24h accumulated precipitation: (a) large-scale condensation removed and (b) convective release of latent heat removed.

other hand, the rain area in Southwest China has also been described correctly. Precipitation area at the middle and upper reaches of the Yellow River has been reproduced in the control simulation but it is wider than the observed and located west of the observed.

On contrast, Fig.4c shows the 24h precipitation simulated from the model without terrain.There presents still a precipitation area in the Yangtze River valley but the Meiyu rainband disappears. Precipitation in western China (upper reaches of the Yangtze and Yellow Rivers) increases significantly. This may be caused by invasion of cold air from west.

5. *Experiments for Physical Processes (Exps.4–6)*

In this subsection, we investigate the relative contribution of some physical processes to the predicted precipitation. Fig.5a is the predicted precipitation in Exp.4 with large-scale condensation removed. In this case the observed rain area in the Yangtze River and the Huaihe River almost disappears. Fig.5b illustrates precipitation results in Exp.5 with convective release of latent heat removed. Precipitation pattern is almost unchanged. In Exp.6, it is found that vertical turbulent exchanges are not so sensitive to the precipitation. We can conclude that the most important factors in this case are large-scale condensation.

6. *Diagnoses of Simulation Results*

Simulation with terrain can really describe Meiyu process. As is well known, Meiyu front is formed by the confluence of cold and warm air and rainfall is associated with water vapour convergence in the lower troposphere. So, temperature advection and convergence region of vapour flux are diagnosed.

Fig. 6a gives temperature advection distribution from FGGE on 9 July at 700 hPa. Cold advection is located north to the Yellow River and warm advection presides in the Yangtze River valley and south of it. Confluence area of warm and cold air is in a position between the Yangtze and the Huaihe Rivers. Fig. 6b is the result of simulation with terrain. It is similar to Fig. 4a and confluence area is located between the Yangtze and Yellow Rivers. Fig. 6c is the result of simulation without terrain and confluence region extends north of the Yellow River. Cold air advection persists northwest of China. This conditon is not favourable for rainfall over the Yangtze and Huaihe River valley.

Fig. 7a gives vapour flux convergence at 700 hPa from 8 July FGGE data. A convergence band extends from Southwest China to the Yangtze and Huaihe River valley. Fig. 7b is the corresponding simulation result with terrain. Convergence region is still located from Southwest China to the Yangtze and Huaihe River valley. Fig. 7c is the simulation

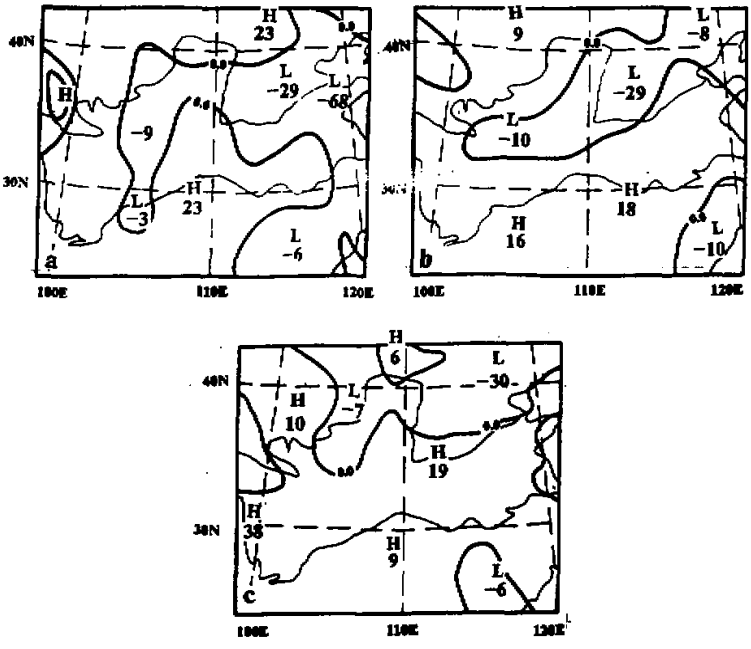

Fig. 6. Temperature advection at 700 hPa: (a) from FGGE on 9 July; (b) simulated from the model with terrain; and (c)simulated from the model without terrain.

result without terrain. The Yangtze and Huaihe River valley has been occupied by a divergence region and the convergence region has migrated north to the Yellow River.

VI. CONCLUSIONS

Highlights and specific findings of the present numerical experiment are summarized:

(1) The Lagrangian scheme can successfully describe Meiyu system and Meiyu precipitation.

(2) Comparative experiments with total terrain, without terrain and with 1 / 3 terrain show that the Tibetan Plateau has a close relation with Meiyu in East Asia. In the experiment with terrain, a clear rainband can be seen presiding at the Yangtze and Huaihe Rivers. Without terrain, the rainband is not found clearly and precipitation area moves westwards. It can be also found that positions of trough and ridge position simulated from the model with terrain are similar to the observed. Without terrain, an intense trough predominates over the Plateau, a ridge presides over the Yangtze and Huaihe River valley and Meiyu is difficult to show up. This means the dynamic effect of the Plateau on Meiyu process can not be neglected.

(3) In this Meiyu case, there is a close relation between the 24h precipitation and the large scale condensation. Release of convective latent heat has also an important effect on rainfall. Vertical turbulence exchange has a relatively less important impact on short time change of Meiyu front.

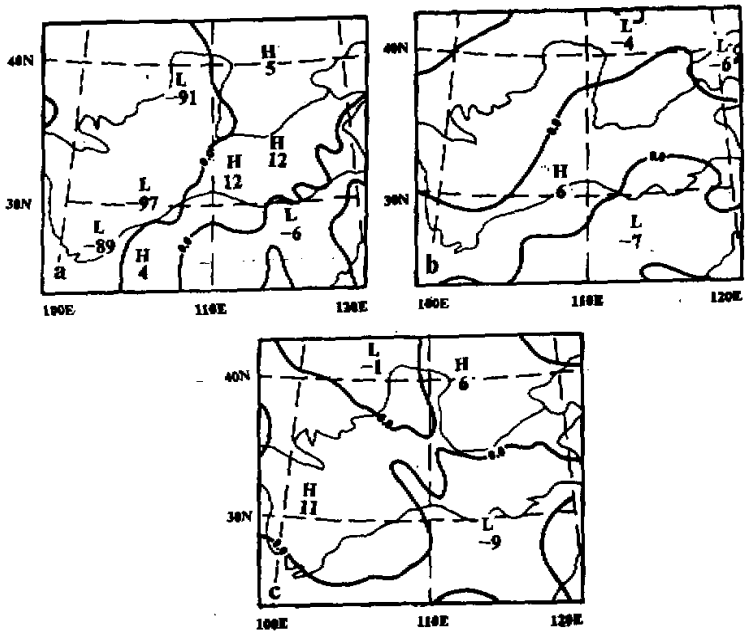

Fig. 7. Vapour flux convergence at 700 hPa (a) from FGGE on 9 July; (b) simulated from the model with terrain; (c) simulated from the model without terrain.

(4) Temperature advection and vapour flux convergence are diagnosed. It is shown that distributions of these physical variables without terrain are quite different from those with terrain. Confluence zone of warm and cold air is located in North China, rather than in the Yangtze and the Huaihe River valley.

To conclude, Meiyu rainband in the Yangtze and Huaihe River valley is related to terrain and Meiyu rainfall is the product of large-scale and convective precipitation. Meiyu front is characterized by both tropic and subtropic systems.

REFERENCES

Anthes, R. A. and T. T. Warner (1978), Development of hydrodynamic models suitable for air pollution and other meteorological studies. *Mon. Wea. Rev.*, **106**: 1045–1078.

Kasahjara, A. and W. M. Washington (1971), General circulation experiments with a six-layer NCAR model, including orography, cloudiness and surface temperature calculation. *J. Atoms. Sci.***28**: 657–701.

Manabe, S. and T. B. Terpstra (1974), The effects of mountains on the general circulation of the atmosphere as identified by numerical experiments, *J. Atoms. Sci.***31**: 3–42.

Muther, M. B. (1983), A quasi-Lagrangian regional model designed for operational weather prediction, *Mon. Wea. Rev.*,**111**: 2087–2098.

Perky, D. J. (1976), A description and preliminary results from a fine-mesh model for forecasting quantitative precipitation, *Mon. Wea. Rev.* **104**: 1513–1526.

Ritchie, H. (1985), Application of a semi-Lagrangian integration scheme to the moisture equation in a regional forecast model. *Mon. Wea. Rev.* **113**: 424–435.

Robert, A., T. L. Yee and H. Ritchie (1985), A semi-Lagrangian and semi-implicit numerical integration scheme for multilevel atmospheric models, *Mon. Wea. Rev.*, **113**: 388-394.

Staniforth, A. and C. Temperton (1986), Semi-implicit semi-Lagrangian integration schemes for a barotropic finite-element regional model, *Mon. Wea. Rev.* **114**: 2078-2090.

Tao, S. Y., et al. (1980), The Heavy Rainfalls in China, Science Press, Beijing.

Wang, B. and I. Orlanski (1987), Study of a heavy rain vortex formed over the Eastern flank of the Tibetan Plateau, *Mon. Wea. Rev.* **115**: 1370-1393.

Ye, D. Z. and Y. X. Gao et. al. (1979), The Meteorology of Qinghai-Xizang (Tibet) Plateau, Science Press, Beijing, 278 pp (in Chinese).

Zhang, Y. L. (1986), Numerical Weather Prediction, Science Press, Beijing (in Chinese).

Zhao, S. X. (1988), The energetics of cyclogenesis on Meiyu (Baiu) front. *Palmen Memorial Symposium on extratropical cyclones, Helsinki Finland*, 205-208.

Zhao, S. X. and G. A. Mills (1991), A study of a monsoon depression bringing record rainfall over Australia Part 2: Numerical predictability experiments, *Mon. Wea. Rev.* **119**: 2053-2073.

Zheng, Q. L. and Liou K. N. (1986), Dynamics and thermodynamics influences of the Tibetan Plateau on the atmosphere in a general circulation model, *J. Atoms. Sci.*, **43**: 1340-1354.

Zhou, X. P., S. X. Zhao, K. S. Zhang and S. H. Liu (1982), Some results of the fine mesh model for numerical forecasting of heavy rainstorm and severe convective storms, *Annual report of Insitute of Atmospheric Physics, Academia Sinica.*, **1**: 251-260.